Diffusion Rates and the Role of Diffusion in Solid Propellant Rocket Motor Adhesion

Kai F. Grythe*, Finn K. Hansen

Department of Chemistry, University of Oslo, N-0315 Oslo, Norway

Received 10 January 2006; accepted 15 July 2006
DOI 10.1002/app.25086
Published online in Wiley InterScience (www.interscience.wiley.com).

ABSTRACT: Diffusion rates can give important information for the adhesion process across the bondline between insulation and propellant in solid propellant rocket motors. Diffusion coefficients of low molecular weight species such as crosslinkers and plasticizers have been measured by the weight of uptake method in polymer materials that are candidates for propellant contact. The materials were EPDM insulation sheets and ''liners,'' based on HTPB, HTPE, or GAP, and with different degrees of particle filling. Plots of relative mass gain as a function of the square root of time showed good linearity up to 20–50% weight increase and the diffusion coefficients could thus be determined with good accuracy. The diffusion coefficients for the low molecular weight isocyanates and plasticizers in these materials vary between 10^{-11} and 10^{-17} m^2 s^{-1}, dependent on material types and particle filling. In most cases, the results can be explained by the solubility parameters of the organic liquids and polymers. For the particle filled samples, the diffusion coefficients decrease with increasing degree of particle filling, and the decrease is faster than predicted by the Maxwell–Fricke or the Keller models for arrays of smooth spheres. © 2006 Wiley Periodicals, Inc. J Appl Polym Sci 103: 1529–1538, 2007

Key words: rocket propellants; diffusion; adhesion; polyurethanes; solubility parameter

INTRODUCTION

Solid rocket motors are insulated thin-walled containers loaded with a solid propellant in which the most important ingredients are an oxidizer and a polymeric binder.[1] In addition, there are a number of additives such as plasticizer, catalyst(s), etc. One major area of concern in the production and storage stability of such motors is the bond between the propellant and the casing insulation. Adhesion failure in the motor can have terrible consequences. Because of the difference in chemical composition of the insulating material and the propellant, the adhesion between these components is a very sensitive function of the material compositions and processing variables such as time, temperature, etc. Some reports are available on how to improve the adhesion between the propellant and the rocket case,[2–8] and Schreuder–Gibson[5] gives a wide background of the adhesion problems in solid rocket motors. Of the more serious problems is migration of components across bondlines that can cause aggravation of bond-line strength. This migration is often an issue with long-time storage of rocket motors, but is also important in the production process of the motor. Diffusion both in the polymer matrix and in the insulation before curing of the propellant is of major importance for the adhesion properties of the system, and in this context the diffusive processes can have both favorable and destructive effects. The diffusion of components such as prepolymers and/or curing agents from the propellant into the insulation material is often a desired process if it results in polymer–polymer interpenetration. According to the diffusion theory of adhesion,[9–12] this will lead to a better bond. However, this diffusion process may also change the NCO/OH molar ratio close to the interface during curing of the polyurethane binder, leading to a region of a cohesively weaker propellant.[13] When a propellant is cast onto the insulation surface, the importance of diffusion of low molecular weight components into the insulation deceases with time during curing of the binder. After the propellant is fully cured, the only mobile component left is usually the plasticizer. Even if long-term stability of the motor casting can be dependent on diffusion of this component, the diffusion during the initial curing period is expected to most strongly affect the strength of the bond.

The migration of components across the bondline is controlled by the mutual diffusion coefficients and the relative solubility of the components in the two phases. In one homogenous phase consisting of n

**Present address:* Nammo Raufoss AS, PO Box 162, NO-2831 Raufoss, Norway.
Correspondence to: F. K. Hansen (f.k.hansen@kjemi.uio.no).
Contract grant sponsors: Norwegian Defense Research Establishment; Nammo Raufoss.

components, there will be $(n–1)^2$ different mutual diffusion coefficients connected to the n individual self-diffusion coefficients and thermodynamic properties of the components.[14] We have in an earlier paper measured the self-diffusion in a binary mixture of the curing agent (diisocyanate) and the prepolymer (polyol) in some important binder formulations.[15] From these data, it is possible to estimate the approximate mutual diffusion coefficients for these binders. In a heterogeneous composite system, the diffusion coefficients will be furthermore affected by the obstruction caused by the filler particles, but the obstruction effect may be calculated for at least moderately filled systems.[16]

The mentioned first study is an initial attempt to obtain relevant data for the assessment of the migration processes in the complex multiphase system of a real rocket motor. In this study, we go a step further to evaluate the diffusion process across the bondline by measuring the diffusion coefficients in the insulation phase. As the molecular weight of the curing agent (diisocyanate) is usually much less that that of the prepolymer, the diffusion of the latter in the insulation material will be very low. In this phase, it is therefore most interesting to investigate the diffusion of the curing agent(s) and the plasticizer, and this article shows that this may be done by the very simple procedure of measuring the weight uptake of the low molecular weight species into the insulation material.

THEORETICAL CONSIDERATIONS

The diffusion of a single substance from the interphase into the isolation may be considered as ordinary diffusion into a semiinfinite slab and is described by Fick's second law of diffusion. If the thickness of the slab is also considered infinite, the concentration C as a function of time, t, is simply[17]

$$C = C_0 \mathrm{erfc} \frac{x}{2\sqrt{Dt}}, \tag{1}$$

where erfc() is the complementary error function. Here C_0 is the concentration at the interphase, x the distance from the interphase into the insulation, and D is the diffusion coefficient. This equation also assumes that there is only one diffusing component and that the diffusion coefficient of this is constant. The flux at the interphase is given by Fick's first law and is thus

$$J = D\left(\frac{dC}{dx}\right)_{x=0} = C_0\left(\frac{D}{\pi t}\right)^{1/2} \tag{2}$$

The flux is the rate of mass transport per unit area, A. If we write the concentration as weight per unit volume, w_0/V, we can write

$$\frac{\mathrm{d}w}{\mathrm{d}t} = AJ = A\frac{W_0}{V}\left(\frac{D}{\pi t}\right)^{1/2}, \tag{3}$$

where w is the weight of the diffusing substance. In a pure liquid, w_0/V is the same as the density, ρ. By integrating eq. (3) from $t = 0$ to some time t_1, we find the total amount of diffused substance, w_1, during this time interval,

$$w_1 = A\rho\left(\frac{Dt_1}{\pi}\right)^{1/2} \tag{4}$$

If we measure the uptake of the diffusing substance as a relative weight increase, we can write

$$\frac{m}{m_0} = \frac{w_1 + m_0}{m_0} = \frac{w_1}{m_0} + 1 = \frac{A\rho}{m_0}\left(\frac{Dt_1}{\pi}\right)^{1/2} + 1, \tag{5}$$

where m is the mass of the isolation sheet including the absorbed substance, and m_0 is the initial mass. If a thin sheet of insulation is swollen by the absorbing liquid, the surface area on both sides must be included, and we can exchange A by $2A_i$, the surface area of the sheet, assuming that the edges can be neglected. In addition, we can multiply both the numerator and denominator by the sheet thickness, d_i. Observing that $A_i d_i = V_i$, the volume of the sheet, and that $m_0/V_i = \rho_i$, the initial density of the sheet, we can write

$$\frac{m}{m_0} = \frac{2\rho A_i d_i}{m_0 d_i}\left(\frac{Dt_1}{\pi}\right)^{\frac{1}{2}} + 1 = \frac{2\rho}{\rho_i d_i}\left(\frac{Dt_1}{\pi}\right)^{1/2} + 1 \tag{6}$$

By plotting the relative weight increase as a function of the square root of time, we should obtain a straight line where the slope is proportional to the square root of the diffusion coefficient, i.e.,

$$\frac{d}{d\sqrt{t}}\left(\frac{m}{m_0}\right) = \frac{2\rho}{\rho_i d_i}\left(\frac{D}{\pi}\right)^{1/2}. \tag{7}$$

Deviations from a straight line can thus be interpreted to indicate a nonconstant diffusion coefficient. We note that the slope will be dependent on the thickness of the sheet. At any time, t_1, an ''average'' D can be calculated from

$$D = \pi\left(\frac{m}{m_0} - 1\right)^2\left(\frac{\rho_i d_i}{2\rho}\right)^2\frac{1}{t_1} \tag{8}$$

This procedure also is only valid at times where a noticeable part of the diffused mass has not yet reached the mid-point of the sheet, after which the gradient will decrease and the absorption rate finally diminish. For a plane sheet like the present geometry, solutions to the diffusion equation also in this more general case

are readily available,[17] and thus the expected time for a decrease in the slope of the plot against the square root of time can be estimated. The exact value of this time will be dependent on when the change in slope will be noticeable by the experimental procedure. We have in this work chosen to use the characteristic time where $Dt/d^2 = 1$, i.e., when

$$t = \frac{d^2}{D} \tag{9}$$

For this condition, the value $C_{d/2}/C_0 = 0.3145$, where $C_{d/2}$ is the concentration at the mid-point, has been calculated.[17] This means for example that for a 1-mm sheet and a diffusion coefficient of 10^{-12} m^2 s^{-1} this characteristic time is 10^6 s, or 278 h. This quite high value indicates that the linearity in the square root of time relationship should be good for many of the measured systems, as will be shown later, even if the saturation effect may be noticed somewhat earlier than at the chosen condition. The linear relationship is also of course only valid as long as the diffusion coefficient is constant.

In some of the measured polymer sheets, particle fillers have been added to simulate composite insulation liners that are often used in rocket motors. Depending on the particle content, the particle size and shape, and on the diffusion coefficient of the penetrant in the particles, the fillers will affect the total diffusion coefficient. This phenomenon has often been called the obstruction effect, and has also been treated quantitatively for different conditions.[17] If the particles are significantly larger than the diffusing molecules, cannot be penetrated, and the degree of filling is less than 70% by volume, this obstruction effect has been described by the so-called Maxwell–Fricke equation.[18] In the case of completely unpenetrated particles, this equation can be expressed as

$$\frac{D'}{D} = \frac{\gamma(1-p)}{\gamma + p} \tag{10}$$

where D' is the observed diffusion coefficient, p is the volume fraction of solid material, and γ is a geometric constant which is 2 for spheres and 1 for cylinders. Many researchers have proposed different expressions for the obstruction effect, both theoretically and numerically computed. The models are usually based on arrays of spheres, cylinders, ellipsoids, or rectangular blocks, and different expressions have been obtained, depending on these conditions. Common to these models is, however, that the calculated obstruction effect is usually larger than that calculated from eq. (10). An expression proposed by Keller[19] is

$$\frac{D}{D'} = -\frac{\pi}{2}\ln\left(\frac{\pi}{6} - p\right) + \ldots, \tag{11}$$

Keller also presented a similar expression for cylinders. We see that D' from eq. (11) decreases more strongly and becomes zero already at $p = \pi/6 = 0.524$ when the spheres touch. In the case of irregular particles, researchers have also found lower diffusion coefficients than for smooth particles of the same shape. It may be concluded that good theories for predicting the obstruction effect in all types of composites do not really exist.

EXPERIMENTAL

The absorption of up to six different liquids has been measured in a number of polymer sheets. The liquids are listed in Table I. The densities have been measured by pyknometry at 22–25°C. Isophorone diisocyanate (IPDI) was obtained from Degussa (Germany) (trade name VESTANAT IPDI). 4,4′ Diphenylmethane diisocyanate (MDI) was obtained from Sika (Switzerland) (SikaForce-7010), and consists of a mixture of isomers and homologous components. Metylenebis(4-cyclohexylisocyanate) (MBCI) (Desmodur W) and hexamethylene diisocyanate (HDI) (Desmodur N-100) were both obtained from Bayer (Germany). Dimeryl diisocyanate (DDI 1410) and dioctylsebacate (DOS) (Edenol 888), was obtained from Cognis (Germany). *N*-butyl-2-nitratoethylnitramine (Bu-NENA) was obtained from Dyno Defense. All chemicals were used as received.

The polymer sheets are listed in Table II. Two samples consist of EPDM rubber that are crosslinked and filled with fibers, flame retardants, and other substances. The two different products have different composition, but the exact composition is not disclosed by the manufacturer. One apparent difference between the two products is that EPDM-R1100 has a higher degree of filling, but does not have a higher density. These two materials are typical insulating materials used to protect the rocket motor case from the motor heat. The rubber composites are manufactured by ATK (Rocket Center, VW) and Trelleborg Viking (Norway), and manufactured into sheets by Nammo Raufoss. During manufacturing, care is taken to evacuate peroxide curing biproducts.

All polymer sheets except for those based on EPDM rubber were made in the lab. A series of polyur-

TABLE I
Molecular Weight (M_n), Polydispersity Index (PI) and Density of the Liquids Used

Substance	M_n	PI	Density at 25°C
IPDI	222.3	1.0	1.061
MDI	327.0	1.7	1.239
DDI	597.9	–	0.924
MBCI	262.3	1.0	1.071
DOS	426.7	1.0	0.913
Bu-NENA	207.2	–	1.227

TABLE II
Materials Tested for Solvent Penetration

Designation	Type	Ca thickness (mm)	Density (g cm^{-3})
EPDM-R1100	EPDM rubber (ATK)	1	1.16
EPDM-VT	EPDM rubber (Trelleborg Viking)	2	1.17
xx-y-zz	Polyurethanes	1–4	–
SR-1	Silicone elastomer, Dow Corning, 93–104	2	1.05
SR-2	Silicone elastomer, Sylgard 170	3	1.37
PES-1	Crosslinked branched polyester, Desmophen 1100 (Bayer)	2	1.07
PES-2	Crosslinked, linear polyester, Baycoll AD 3040 (Bayer)	2	1.02
PU	SikaForce-7710 L100	2	1.50
EP	Eccobond (Emerson and Cuming), epoxy	3	1.31

ethanes were made based on three different prepolymers and cured with three different diisocyanates. As prepolymers, hydroxyl terminated polybutadiene (HTPB) (R45HT; Elf Atochem), glyzidyl azide polymer (GAP) (SNPE), and hydroxyl-terminated polyethylene glycol (HTPE) (ATK) were used. The diisocyanates used were IPDI, MDI, or HDI. Such polyurethanes are usually referred to as ''liners'' by the rocket motor industry; they can be used as insulation, but also as a part of the bonding system. Therefore, they are often called bond-liners. Often, liners are mixed with solid particles to improve the mechanical and rheological properties. These particles also give an obstruction effect on the diffusion rates in the liner; as will be discussed later in this article. The series of polyurethane liners are coded xx-y-zz. The code xx denotes the polymer type, PB = HTPB, PE = HTPE, or GP = GAP, y denotes the filling agent, C = carbon black (CB) or T = TiO_2, and zz is equal to the percentage (w/w) of the filling agent. Carbon black thermax was obtained from Cairn Chemicals Ltd., and TiO_2 from Kronos (Norway). Detailed composition of the liners can be found in Table III.

SR-1 and SR-2 are two-part silicone elastomers (Dow Corning Corp.), SR-1 is fiber-filled and SR-2 is not. Approximately 2-mm thick sheets were made from these polymers by curing for 24 h at 25°C. The sheets denoted PES-1 and PES-2 were produced by mixing polyester prepolymer and a crosslinker (MDI) in a beaker and pouring this mixture into a dish. The ratio prepolymer/curing agent of 2.5/1 was used for PES-1 and 9/1 for PES-2. The mixtures were evacuated to remove air bubbles. After crosslinking at ambient temperature for 5 days, the polymer was cut into rectangular pieces. The polymer denoted with PU is a two-component polyurethane adhesive with MDI as the curing agent and with particle fillers. EP denotes a two component epoxy adhesive, often used as a barrier for inhibiting migration in binding systems. For all materials except the two EPDM samples, the densities were calculated from the respective densities of the ingredients. For the two EPDM samples, the densities were measured by weight measurement in *n*-hexane. Thickness could vary between samples, but the exact thickness was always measured for use in calculations. All samples except SR-1, SR-2, PES-1, PES-2, and PU were cured at 60°C. The curing time is shown in Table VI.

The absorption experiments were performed by submerging a piece of polymer sheet in liquid. The size of the sample was $\sim 10 \times 20$ mm^2 and thickness 1–3 mm. The sample was weighed initially and then at regular time intervals, up to 14 days. At each weighing, the sample was carefully dried to remove excess liquid, and weighed immediately to avoid loss. The sample was then reimmerged in the liquid. The samples were kept at room temperature in closed containers. The thickness was measured at the start and end of the experiment. All reported values are the average of two samples.

RESULTS AND DISCUSSION

The self diffusion coefficients of the pure liquids that were used in the adsorption measurements have been measured by Fourier Transform Pulsed Gradient Spin-Echo NMR (FT-PGSE NMR). The methodology is sim-

TABLE III
Details in the Composition of the Polyurethane Liners

Liner series	Polymer	Curing agent	Ratio of polymer/ curing agent	Curing catalyst % (w/w)	Other ingredients < 1% (w/w)
PB	HTPB	IPDI	5.1	TFB (<1)	Maleic anhydride and MgO
PE	HTPE	HDI	7	DBDTL (<0.01)	–
GP	GAP	HDI	4.4	DBDTL (<0.01)	–

TABLE IV
Self-Diffusion Coefficients from FT-PGSE Measurements

Substance	D_{SE} ($m^2\ s^{-1}$)	β	D_S ($m^2\ s^{-1}$)
IPDI	6.39×10^{-11}	0.99	6.36×10^{-11}
MDI	4.34×10^{-12}	0.84	3.95×10^{-12}
DDI	4.54×10^{-12}	0.98	4.50×10^{-12}
MBCI	2.37×10^{-11}	0.98	2.35×10^{-11}
DOS	3.51×10^{-11}	0.99	3.49×10^{-11}
BuNENA	3.52×10^{-11}	0.98	3.49×10^{-11}

ilar to that used in earlier work and is described elsewhere.[15] Measured self diffusion coefficients are given in Table IV. All substances have been fitted with a stretched exponential function using the Origin program, but as can be seen from Table IV, only MDI have a distribution of diffusion coefficients (i.e., $\beta < 1$). The other substances have β values very close to 1, indicating a single diffusion coefficient and one diffusing specie. IPDI is the fastest diffusing specie, about twice as fast as MBCI, DOS, and BuNENA. MDI and DDI are considerably slower, having about 10 times lower diffusion coefficients. (The measured self diffusion coefficient for IPDI is higher than reported in earlier work,[15] $5.04 \times 10^{-11}\ m^2\ s^{-1}$, the most probable reason for this is a temperature rise in the NMR instrument.) Self diffusion coefficients do not easily relate to mutual diffusion coefficients[14,15] and in the solvent uptake experiments, the mutual diffusion coefficients are measured. However, the self diffusion coefficients give a basis for the estimation of mutual diffusion coefficients, especially when correlated with thermodynamic parameters such as solubility parameters, as will be shown later.

As explained in the theoretical part, if the relative absorption, i.e., weight increase m/m_0, is plotted as a function of the square root of time, a straight line is expected as long as the diffusion coefficient is constant and the diffusing substance has not to a noticeable

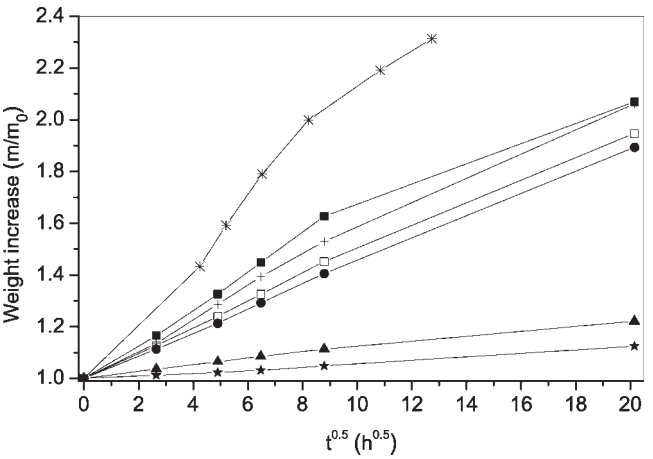

Figure 2 Relative absorption IPDI 2.8 mm thick (■), IPDI 4.1 mm thick (□), MDI (●), DOS (▲), DDI (★), MBCI (+), and BuNENA (∗) in PE-0 as function of the square root of time.

degree reached the middle of the sheet interior. Since the sample thickness was variable to some degree, slopes read from the plots cannot always be compared directly, but useful information can be extracted and the diffusion coefficient can be calculated from the linear parts. A representative selection of results is plotted in Figures 1–6, where data for the weight increase with 6–7 low-molecular weight substances are plotted for some polymer materials. These materials were selected to represent well the different material types investigated. For adsorption of the prepolymers no significant weight increase could be measured even after 2 weeks.

Generally, most of the plots are quite linear, a fact that indicates constant diffusion coefficients quite far into the absorption process. At longer times, a decrease in the rate of uptake is seen for some of the liquids in some solids. The most probable reason for this is the saturation of the sample with the liquid, an

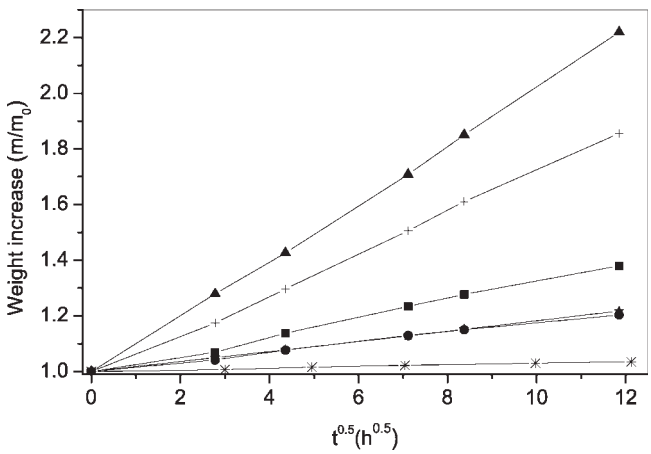

Figure 1 Relative absorption IPDI (■), MDI (●), DOS (▲), DDI (★), MBCI (+), and BuNENA (∗) in PB-0 as function of the square root of time.

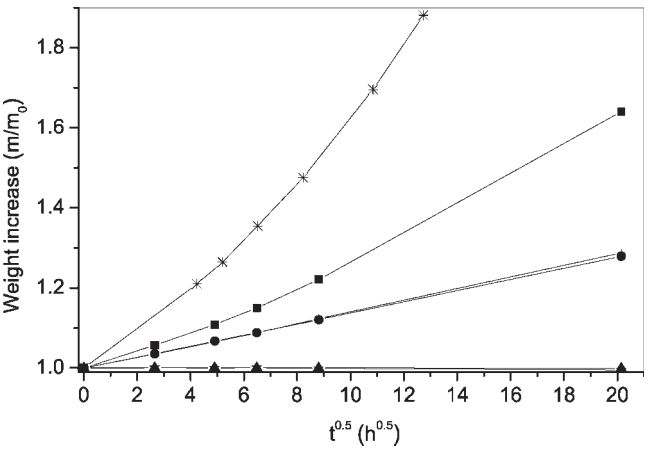

Figure 3 Relative absorption IPDI (■), MDI (●), DOS (▲), DDI (★), MBCI (+), and BuNENA (∗) in GP-0 as function of the square root of time.

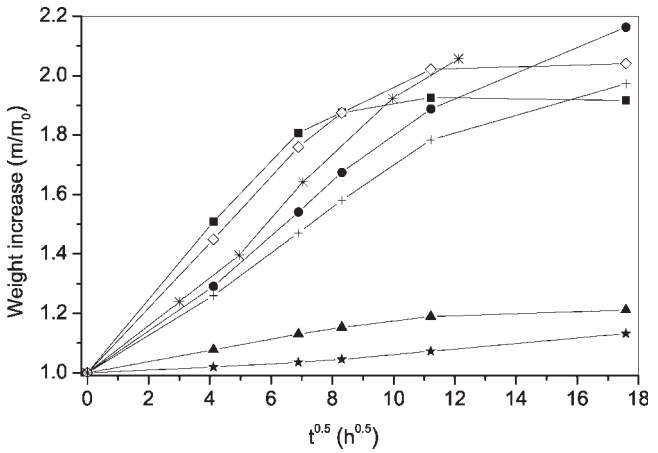

Figure 4 Relative absorption of IPDI (■), MDI (●), DOS (▲), DDI (★), MBCI 2.3 mm thick (+), MBCI 1.4 mm thick (◇), and BuNENA (*) in PE-C-10 as function of the square root of time.

assumption that is confirmed by the fact that the slow-down is mostly observed at high values of m/m_0 > ca. 1.5. The time for the start of this process can be estimated as explained in the theoretical part, e.g., from eq. (9). It is noted that the time calculated from this equation is dependent on the sample thickness. The calculation of the diffusion coefficients is based on the slopes at 36-h diffusion time ($\sqrt{t} = 6$), so as to avoid saturation in most cases. The results are shown in Table VI. They are calculated according to eq. (8), using the densities of the liquid phase given in Table I, and the density of the solids from Tables II and VII.

Examples of the saturation effect are seen in Figures 4 and 5. The slope of the $\sqrt{t}$-relationship of MBCI, IPDI, and MDI is decreasing after a given time. For IPDI in Figure 4, the bend is observed after $\sim$ 50 h and beyond $\sim$ 100 h there is no further weight increase. The diffusion coefficient for IPDI calculated for this case is 5×10^{-12} m^2 s^{-1}, and with a sample thickness of 1.2 mm, the time calculated from eq. (9) is 80 h. For MBCI in the same figure, the diffusion coefficient is 5.5×10^{-12} m^2 s^{-1} and the times calculated from eq. (9) are 99 and 267 h for the 1.4- and 2.3-mm thick samples, respectively. This fits fairly well with the observed data, especially taking into consideration the approximate nature of the condition for eq. (9) and the relatively long time intervals between the data points. As this determination has not been the main objective of this work, a more accurate determination of the time for saturation has not been done. It may be concluded that the change in slope most probably is due to material saturation.

A general tendency in many of these plots is the slight increase in slopes at early times. These observations are uncertain because of larger measurement errors at these low swelling ratios. In the plots shown, this can be seen in Figure 5 for DOS and MBCI in EPDM-R1100, and in less extend for IPDI in PE-C-10 in Figure 4. This increase in slope would mean an increase in diffusion coefficients, which may be possible if a swelling of both surface and bulk material can make further diffusion across the surface and into the bulk material easier, due to a more open network structure. Such an increase might be expected to be a general phenomenon in all these materials, but so does not seem to be the case; it seems rather to be limited to the material R1100 at swelling ratios below ca. 10%. This may be caused by the special fiber-filled structure of this material.

An error in all calculations of diffusion coefficients is the assumption that the thickness of the insulation, and thereby the x-coordinate, is constant during the measurements. The thickness is increasing with time, and after 64 h the thickness has increased by ca. 2–10%, depending on the rate of diffusion. This error is considered small when compared with other errors such as reproducibility of material crosslinking, homogeneity, etc., and is therefore ignored.

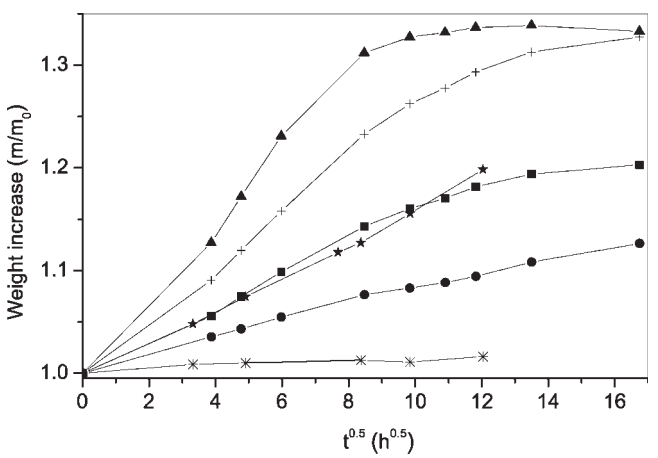

Figure 5 Relative absorption of IPDI (■), MDI (●), DOS (▲), DDI (★), MBCI (+), and BuNENA (*) in EPDM-R1100 as function of the square root of time.

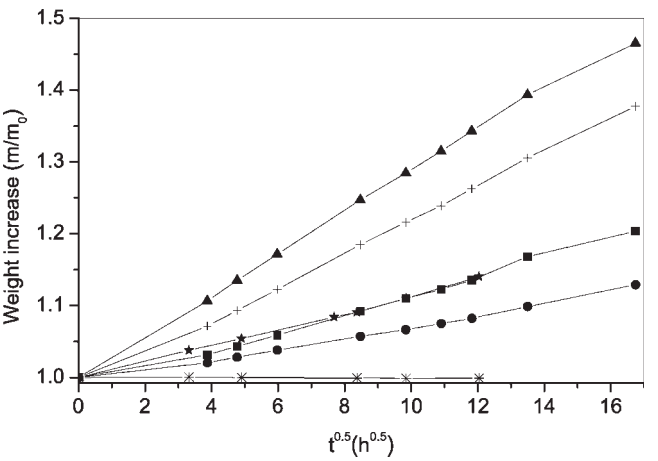

Figure 6 Relative absorption of IPDI (■), MDI (●), DOS (▲), DDI (★), MBCI (+), and BuNENA (*) in EPDM-VM as function of the square root of time.

From the results, it is clear that the diffusion coefficients for all substances, except BuNENA, are higher in EPDM-VT than in EPDM-R1100, even if this is the same type of filled EPDM material. This is, however, not surprising, given the higher degree of particle filling of the latter. It is interesting to note that the difference between the two is not the same for all substances, even if the diffusion coefficients in EPDM-VT are roughly the double of those in R1100.

The polymers SR-1, SR-2, PES-1, PES-2, and PU have been measured only in IPDI and MDI. Except PES-2, they all have very low diffusion coefficients for these two liquids, almost as low as EPX, which can be characterized as a barrier. Diffusion coefficients can be measured in EPX, but they are low enough that the diffusion for practical purposes can be neglected. PES-2 is based on a linear, crosslinked polyester, and the higher diffusion coefficient compared with the branched PES-1 may be explained by a more open network structure.

The magnitude of the diffusion coefficients does not follow the molecular weights. DOS has the highest diffusion coefficients in the PB series, even if DOS has a higher molecular weight that most of the other liquids. But in addition to the molecular weight, both the molecular structure and through that the thermodynamic interaction (''solubility'') in the material will influence the diffusion coefficient. This is very apparent for BuNENA, which is the fastest diffusing liquid in PE and GP systems, while it is the slowest diffusing specie in PB systems. Solubility of organic liquids in polymers is often expressed through the difference in solubility parameters. The solubility parameter for a substance i, δ_i, is defined as the square root of the cohesive energy density and expressed by

$$\delta_i = \left(\frac{\Delta E_i^v}{V_i}\right)^{0.5} \tag{12}$$

where ΔE_i^v is the energy of vaporization and V_i the molar volume. The single solubility parameter describes the attractive strength between the molecules in the material, and mutual solubility between two substances is improved by the minimizing the difference $\Delta_{12} = (\delta_1 - \delta_2)^2$.[20,21] Solubility is, in addition, dependent on the entropy of mixing, and thus also by the molecular weights.

To estimate the solubility parameter for our components, we have used the group contribution method described in the litterature.[21] The method is based on the assumption that the contributions of the different functional groups to the thermodynamic property are additive. The solubility parameter can then be calculated by the expression

$$\delta_i = \frac{\rho_{ij} \sum_j F_j}{M_i} \tag{13}$$

where ρ_i is the density of the component, M_i the molecular weight, and F_j is the molar attraction constant. We have used the attraction constants derived from vapor pressure measurements by Hoy,[22] since they are covering most of the functional groups present in our species. The only exception is for the $—NO_2$ group, which is taken from Small,[23] derived from measurements of the heat of vaporization. The solubility parameter values were calculated for all liquids used in the experiments, and for HTPB, HTPE, and GAP. The results are given in Table V. For GAP, we could not find an attraction constant for the azide group, and the solubility parameter is from Eroglu et al.[24]

If we compare the PB and the PE series in Table VI, DOS and DDI have lower diffusion coefficients in the PE series, while IPDI and MDI have higher diffusion coefficients in the PE series. If we compare the PB and the GP series, DOS and DDI have much smaller diffusion coefficients in the GP series, while they in IPDI and MDI are about the same. DOS is a typical plasticizer used in rocket propellants and is less polar than most of the isocyanates.[25] If we compare the solubility parameters in Table V, the difference Δ_{12} is 0.3, 3.5, and 28.3 for the systems DOS/HTPB, DOS/HTPE, and DOS/GAP, respectively, and the mutual solubility will therefore decrease correspondingly in this series. From Table VI, it is seen that the diffusion coefficient of DOS in these three systems (e.g., PB-0, PE-0, and GP-0) follows the same sequence; it is much lower in HTPE-based materials than in HTPB-based, and practically zero in GAP-based materials. The same dependency can be observed for DDI. The liquids MBCI and IPDI have very similar solubility parameters as HTPE, and both have higher diffusion coefficients in PE than in PB polymers.

In Figure 7, the diffusion coefficients are plotted for each liquid against the difference Δ_{12} for nonfilled PB, PE, and GP. It is seen that the correlation is good for some liquids, but less so for others. There is a clear tendency that solvent systems where the solubility parameter is much different from that of the polymer also have a very low diffusion coefficient in that poly-

TABLE V
The Solubility Parameter for the Isocyanates, Plasticizers, and Some of the Polymers

Substance	δ (MPa)$^{0.5}$
DOS	16.65
DDI	16.69
HTPB	17.19
IPDI	17.94
MBCI	18.76
HTPE	19.07
MDI	22.09
GAP	22.51
Bu-NENA	22.55

TABLE VI
Calculated Diffusion Coefficients According to eq. (8) After 36 h

Material designation	Curing time (h)	IPDI (10^{13} m^2 s^{-1})	MDI (10^{13} m^2 s^{-1})	DDI (10^{13} m^2 s^{-1})	MBCI (10^{13} m^2 s^{-1})	DOS (10^{13} m^2 s^{-1})	BuNENA (10^{13} m^2 s^{-1})
PB-0	168	9.7	2.6	6.6	52.1	130	0.085
PB-C-10	96	7.2	1.7	2.4	28	75	–
PB-C-20	72	3.1	1.7	1.8	30	26	0.041
PB-C-40	96	3.3	1.1	1.3	9.6	23	–
PB-T-10	120	7.1	3.3	4.8	26	85	–
PB-T-20	96	8.3	2.6	3.5	31	70	–
PB-T-40	96	6.5	2.7	2.2	20	50	–
GP-0	96	5.6	3.8	< 0.001	4.0	< 0.001	29
GP-C-20	72	3.1	1.6	~ 0.0004	1.4	~ 0.0002	17.1
PE-0	96	82	44	0.49	80	7.5	91
PE-C-10	20	50	27	0.39	55	4.9	86.8
PE-C-20	72	37	29	0.39	40	3.5	72.8
PE-C-40	96	58	33	0.46	60	3.9	93
SR-1	24[a]	< 0.001	< 0.001	–	–	–	
SR-2	24[a]	< 0.001	0.081	–	–	–	–
PES-1	24[a]	~ 0.001	~ 0.001	–	–	–	–
PES-2	24[a]	3.0	3.6	–	–	–	–
PU	24[a]	0.058	0.029	–	–	–	–
EPDM-R1100	–	0.69	0.16	0.63	2.6	5.2	0.0067
EPDM-VT	–	1.1	0.35	1.5	4.7	13	<0.001
EPX	48	0.0024	0.0029	0.0063	0.0015	0.0035	0.0076

[a] Cured at room temperature.

mer. There are two major deviations from this relationship. Firstly, MDI and BuNENA have a much lower diffusion coefficient in GP systems and secondly, IPDI have a much lower diffusion coefficient in PB than expected from the Δ_{12} difference. However, in addition to the pure solubility effect, the degree of crosslinking of the polymers also influences the diffusion coefficients (through the free volume). Some of the observed deviations, especially for the GP polymer, may therefore be explained by a denser network structure. Since the deviations seem to exist especially at low Δ_{12}, it indicates that the effect of the network structure is most noticeable when the solubility is good, and at lower solubility, with lower diffusion rates, the effect of the network structure is less important. The number of data points is, however, too low to draw this conclusion with any certainty. Since the polymers in which the diffusion coefficients have been measured are cured with IPDI (for PB) and HDI (for PE and GP), the solubility parameter for the polymer material may not be the same as the solubility parameter of the prepolymers. Using the group contribution method, the solubility parameter can be estimated to 21.0 MPa$^{0.5}$ for the type of HDI used. This may indicate that the actual solubility parameter for GP polymer is a little bit lower than for GAP, and for PE polymer a little bit higher than for HTPE.

It is interesting to note that compared with the self-diffusion coefficients we have measured in polyol/diisocyanate mixtures, these diffusion coefficients are considerably, 1–2 orders of magnitude, lower. This means that it is possible to simulate the migration of low molecular substances from the propellant into the insulation sheet, by assuming, as a first approximation, that the concentration in the propellant phase is constant. The effect of the different composite fillers on the diffusion coefficient in these materials is given in Table VII. As can be seen from this table, the measured diffusion coefficients decrease in most cases faster than predicted by either the Maxwell–Fricke or the Keller models for arrays of smooth spheres. In case of cylinders, the models predict somewhat stron-

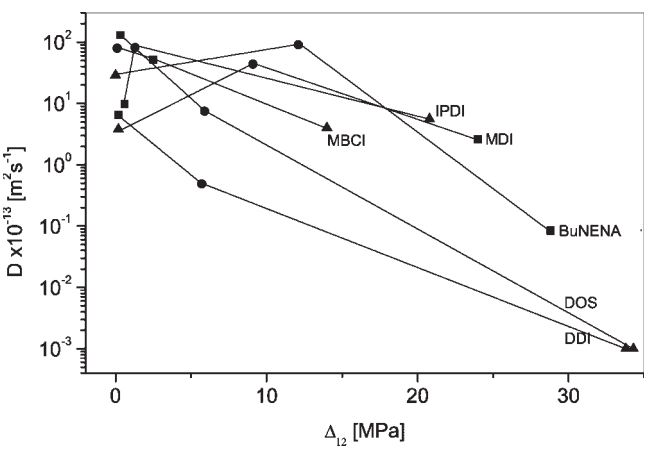

Figure 7 The diffusion coefficient for different liquids in PB-0 (■), PE-0 (●), and GP-0 (▲), plotted as function of the square root of the difference between the solubility parameters for the liquid and the polymer.

TABLE VII
The Effect of Fillers on the Diffusion Coefficient (D/D_0)

Liner	Calculated density (g cm^{-3})	Volume fraction solids	IPDI	MDI	DDI	MBCI	DOS	BuNENA	Fricke (spheres)	Keller (spheres)
PB-0	0.945	0	1	1	1	1	1	1	1	1
PB-C-10	1.01	3.8	0.74	0.68	0.36	0.54	0.58	–	0.94	0.87
PB-C-20	1.09	8.3	0.32	0.68	0.27	0.58	0.20	0.48	0.88	0.78
PB-C-40	1.27	19.4	0.34	0.44	0.20	0.18	0.18	–	0.73	0.58
PB-T-10	1.02	2.5	0.73	1.32	0.73	0.50	0.65	–	0.96	0.91
PB-T-20	1.12	5.4	0.86	1.04	0.53	0.59	0.54	–	0.92	0.84
PB-T-40	1.37	13.3	0.67	1.08	0.33	0.38	0.38	–	0.81	0.68
GP-0	1.26	0	1	1	1	1	1	1	1	1
GP-C-20	1.41	10.7	0.55	0.42	~ 1	0.35	~ 1	0.59	0.85	0.73
PE-0	1.06	0	1	1	1	1	1	1	1	1
PE-C-10	1.13	4.3	0.61	0.61	0.80	0.69	0.65	0.95	0.94	0.87
PE-C-20	1.21	9.2	0.45	0.66	0.80	0.50	0.47	0.80	0.87	0.76
PE-C-40	1.40	21.2	0.71	0.75	0.94	0.75	0.52	1.02	0.71	0.54

ger obstruction effects (not shown), but also in this case the experimental effect is stronger. It has been concluded earlier that good general theoretical models for predicting obstruction effects in composite materials do not exist, and our data seem to confirm this observation. There is some variability in the measured values that is most probably due to errors both in the reproducibility of materials and in the measurements themselves. This variability makes it difficult to reach clear conclusions, but carbon black is clearly a more efficient barrier against diffusion than TiO_2 particles. It is well known that carbon black has a very high specific surface, and it is tempting to correlate its barrier properties with this surface. It is also known that porous materials slow down diffusion both through a size exclusion effect and by specific adsorption, as in chromatographic processes. This again means that the diffusion through a filled material can also be dependent on the specific interactions between the particle surface and the diffusing material, and that different fillers therefore will have different effects on diffusion. The observed effects may be explained on this background.

When it comes to prevent diffusion across the interphase, with subsequent possible curing problems in the propellant, these data can be used to consider if the use of a dedicated barrier like EPX is necessary. Depending on the components present in the propellant system of interest, these data can give guidelines to designing the bonding system. For example, if silicone rubbers are used, the diffusion of IPDI is of no concern, but in other systems, like EPDM systems, the diffusion of IPDI may cause problems. DDI used in GP systems is another example of a system where we have approximately no diffusion of the curing agent. Also, when it comes to diffusion over a longer time scale, i.e., diffusion of plasticizer over a time scale of several years, DOS in PB-systems may cause problems, while DOS in GP systems is of much less concern. BuNENA in PB-systems is also of less concern, while care must be taken in the use of BuNENA in GP and PE systems to avoid problems.

CONCLUSIONS

The simple methodology of measuring the weight uptake of the low molecular weight species into the insulation materials can be successfully used to calculate diffusion coefficients of the species. Diffusion coefficients between 10^{-11} and 10^{-17} m^2 s^{-1} have been obtained, and this huge span in diffusion properties shows the importance of taking diffusion into account when designing propellant/bonding systems. It is often assumed that some degree of diffusion across the interphase promotes adhesion according to the diffusion theory of adhesion, but that too high degree of intermixing will cause curing problems by changing the stochiometry, i.e., the hydroxyl/isocyanate ratio. The measured diffusion coefficient may contribute significantly to the understanding of the complex migration processes in a solid propellant rocket motor.

Particle fillers in the solid materials will lower the diffusion coefficients, which has also been measured in this work. However, this effect is found to be larger than predicted by both the Maxwell–Fricke and the Keller models. In the present experiments, carbon black was a more efficient barrier against diffusion than TiO_2 particles, possibly because of its higher specific surface and/or adsorbent properties. The difference in solubility parameters calculated from the group contribution method can partly be used to explain the large differences observed in the diffusion coefficient of the different species in the materials, while an additional factor may be a variable degree of crosslinking in the different materials.

We thank Torbjørn Olsen at the Norwegian Defense Research Establishment and Jon Huse at Nammo Raufoss for general help with chemicals and discussions, and Eddy Walter Hansen for giving access to the NMR equipment.

References

1. Davenas, A., Ed. Solid Rocket Propulsion Technology; Pergamon: Oxford, UK, 1993.
2. Haska, S. B.; Pekel, F. Presented at the 26th International Annual Conference of ICT, Karlsruhe, Germany, 1995.
3. Haska, S. B.; Bayramli, E.; Pekeland, F.; Ozkar, S. J Appl Polym Sci 1997, 64, 2347.
4. Sanden, R.; Wingborg, N. J Appl Polym Sci 1989, 37, 167.
5. Schreuder-Gibson, H. L. Rubber World 1990, 203, 34.
6. Gottlieb, L.; Bar, S. Propellants Explosives Pyrotech 2003, 28, 12.
7. Giants, T. W. Case Bond Liner Systems for Solid Rocket Motors; Materials Science Lab, Aerospace Corporation, El Segundo, CA, 1991.
8. Hemminger, C. S. Presented at the 33rd AIAA/ASME/SAE/ASEE Joint Propulsion Conference and Exhibit, Seattle, WA, 1997.
9. Voyutskii, S. S.; Vakula, V. I. Rubber Chem Technol 1964, 37, 1153.
10. Jabbari, E.; Peppas, N. A. J Macromol Sci Rev Macromol Chem Phys 1994, 34, 205.
11. Pocius, A. V. Adhesion and Adhesives Technology: An Introduction; Hanser: Munich, 2002.
12. Ruch, F.; David, M. O.; Vallat, M. F. J Polym Sci Part B: Polym Phys 2000, 38, 3189.
13. Grythe, K. F. Study of the Interface between Insulation and Propellant in Solid Propellant Rocket Motors; NTNU: Trondheim, Norway, 2002.
14. Tyrell, H. J. V.; Harris, K. R. Diffusion in Liquids; Butterworths: London, 1984.
15. Grythe, K. F.; Hansen, F. K.; Walderhaug, H. J Phys Chem B 2004, 108, 12404.
16. Amsden, B. Macromolecules 1999, 32, 874.
17. Crank, J. The Mathematics of Diffusion; Clarendon: Oxford, 1975.
18. Fricke, H. Phys Rev 1924, 24, 575.
19. Keller, J. B. J Appl Phys 1963, 34, 991.
20. Krevelen, D. W. V. Properties of Polymers; Elsevier: Amsterdam, 1990.
21. Grulke, E. A. Solubility Parameter Values; Brandup, J.; Immergut, E. H.; Grulke, E. A., Eds.; Wiley: New York, 1999.
22. Hoy, K. L. J Paint Technol 1970, 42, 115.
23. Small, P. A. J Appl Chem 1953, 3, 71.
24. Eroglu, M. S.; Baysa, B. M.; Gueven, O. Polymer 1997, 38, 1945.
25. Grythe, K. F.; Hansen, F. K. Langmuir, to appear.